THE JOURNAL OF PHYSICAL CHEMISTRY C

Article

Cite This: J. Phys. Chem. C 2018, 122, 15133−15139

pubs.acs.org/JPCC

Photoluminescence Flickering of Micron-Sized Crystals of Methylammonium Lead Bromide: Effect of Ambience and Light Exposure

Ansuman Halder,[†,§] Nithin Pathoor,[‡,§] Arindam Chowdhury,[*,‡] and Shaibal K. Sarkar[*,†]

[†]Department of Energy Science and Engineering and [‡]Department of Chemistry, Indian Institute of Technology Bombay, Powai, Mumbai 400076, India

Supporting Information

ABSTRACT: Recent reports on temporal photoluminescence (PL) intensity fluctuations (*blinking*) within localized domains of organo-metal lead halide (hybrid) perovskite microcrystals have invoked considerable interest to understand their origins. Using PL microscopy, we have investigated the effect of atmospheric constituents and photoillumination on spatially extended intensity fluctuations in methylammonium lead bromide ($MAPbBr_3$) perovskite materials, explicitly for micrometer (ca. 1−2 μm)-sized crystals. Increase in the relative humidity of the ambience results in progressive reduction in the PL intensity, and beyond a threshold value, individual microcrystalline grains exhibit multistate PL intermittency (*flickering*), which is characteristically different from quasi two-state blinking observed in nanocrystals. Such flickering disappears upon removal of moisture, accompanied by considerable enhancement of the overall PL efficiency. We hypothesize that initiation of moisture-induced degradation marked by the lowering of PL intensity correlates with the appearance of PL flickering, and such processes further accelerate in the presence of oxygen as opposed to an inert (nitrogen) environment. We find that the intrinsic defects not only increase the threshold level of ambient moisture needed to initiate flickering but also modulate the nature of PL intermittency. Our results therefore establish a strong correlation between initiation of material degradation and PL flickering of hybrid perovskite microcrystals, induced by transient defects formed via interaction with the ambience.

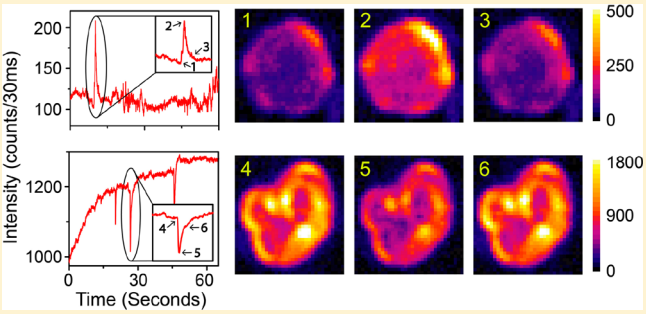

INTRODUCTION

In recent years, hybrid halide perovskite materials, owing to its favorable optoelectronic properties, have evolved as an emerging photon-harvesting material for low-cost photovoltaic devices. Within a relatively short span of time, an unprecedented improvement in the energy conversion efficiency was documented.[1] However, as a major bottleneck to its commercial viability, long-term stability is a major concern in these materials.[2] Extrinsic effects that are often aided by photogenerated charge carriers endorse chemical changes in the materials.[3] Photoluminescence (PL), being sensitive to the disorder in the materials, is well-explored to understand the broader photophysical properties of the particulate films or devices. In addition, PL microscopy provides exclusive information about spatially resolved heterogeneity in the materials.[4] Here, the local information, be it chemical or electronic disorders, in the material can be well-apprehended.[5,6]

Photoexcited charge-carrier recombination dynamics is widely discussed in nanomaterials owing to the high-frequency temporal fluctuation, often termed as *blinking*.[7−9] Here, nonradiative Auger recombination plays a deterministic role because of the high surface-to-volume ratio. In hybrid halide perovskite materials, temporal fluctuation in the PL intensity is observed not only in smaller dimension particles[7,10] but also in aggregates[11] and submicron size grains.[6] In larger size particles (≥few microns), such fluctuation in PL intensity is found in spatially localized domains.[6] Thus, it is obvious that the Auger process may not be the dominant mechanism, rather dynamic traps can also be responsible for PL fluctuation in microcrystals, as argued by Merdasa et al.[5] However, the electronic nature or the formation of these dynamic traps is yet to be understood.

We have previously demonstrated localized PL intermittency within isolated perovskite grains of few microns in a laboratory environment (not controlled).[6] During the course of our measurements, we found that the occurrence of this PL intensity fluctuation of the submicron size crystals varies from sample to sample. Such discrepancies motivate us to understand the effect of the environmental elements that may get involved in the initiation of such a phenomenon. Hence, in this article, we aim to demonstrate a distinct

Received: April 24, 2018
Revised: June 12, 2018
Published: June 14, 2018

DOI: 10.1021/acs.jpcc.8b03862
J. Phys. Chem. C 2018, 122, 15133−15139

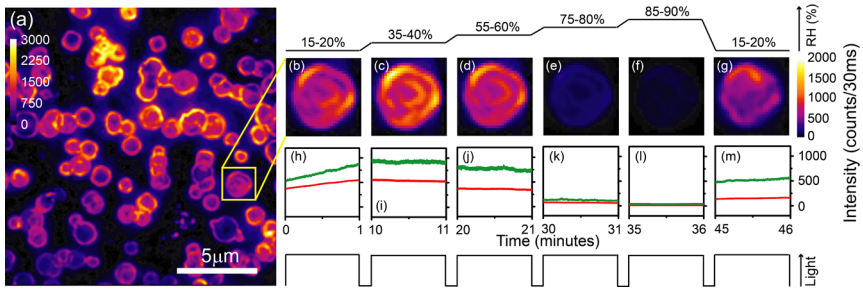

Figure 1. Effect of moisture (in air) on the PL intensity of $MAPbBr_3$ microcrystals. (a) Typical average intensity image of $MAPbBr_3$ microcrystals recorded at 15−20% RH. (b−g) Average PL image of a microcrystal marked with a yellow box in (a) under abovementioned humidity conditions. (h−m) Change in the PL intensity time traces of that particular microcrystal (green) and average PL intensity time traces of the whole ensemble of microcrystals (red) under those RH conditions. The schematic of change in the RH and incident light *on* and *off* condition [intermittent illumination (II)] throughout the experimental time period is shown on the top of the PL images and the bottom of the PL time traces, respectively.

correlation between the surrounding ambience and PL intensity fluctuation in methyl ammonium lead bromide ($MAPbBr_3$) microcrystals.

EXPERIMENTAL METHODS

Synthesis of Methylammonium Bromide. Methylammonium bromide is synthesized by reacting equimolar concentration of methylamine and hydrobromic acid in ethanol (as a solvent) in a round-bottom flask. The solvent is evaporated using a rotary evaporator. The dried powder product is again dissolved in ethanol and recrystallized to from diethyl ether. The recrystallized methylammonium bromide salt is washed repeatedly using diethyl ether and dried in a vacuum oven at 60 °C for 12 h.

Preparation of Microcrystals. A precursor solution of methylammonium lead bromide (0.2 M, $MAPbBr_3$) is prepared from an equimolar mixture of methylammonium bromide and lead bromide (Sigma-Aldrich) in *N*,*N*-dimethylformamide (Sigma-Aldrich) solvent. To form the microcrystals, the precursor solution is spin-coated on a glass coverslip (Fisher Scientific, 25 × 25 × 1 mm) at 2000 rpm for 60 s and annealed at 90 °C for 2.5 min in a nitrogen-filled glovebox. The formation of the material is confirmed by X-ray diffraction and ultraviolet−visible (UV−vis) spectroscopy (Figures S1 and S2).

Material Characterization. The UV−vis−near-infrared absorption measurements were performed using a PerkinElmer LAMBDA 950 spectrophotometer, and the PL measurements were carried out on a JASCO FP-8200 fluorescence spectrometer. The scanning electron microscopy (SEM) images of microcrystals were obtained from a Zeiss Ultra 55 FE-SEM scanning electron microscope from Oxford Technologies.

PL Microscopy of Perovskite Microcrystals. Spatially resolved emission spectroscopy was performed on a home-built wide-field laser epi-fluorescence microscope (Nikon Eclipse 2000U), details of which can be found elsewhere. In brief, the emission from the microcrystals grown on the coverslip is visualized by exciting a large area (~400 μm^2) of the sample with a 405 nm diode laser (LaserGlow, model: LRD-0405-PFR) through an oil immersion objective (Nikon TIRF 1.49NA60X oil) with 1 W cm^{-2} excitation power density. The same objective lens was used to collect the emitted light, which was passed through the necessary dichroic mirror and emission filters, and imaged using an interline charge-coupled device camera (DVC Co. 1412AM). PL movies were collected as 16-bit image sequences at 30 Hz (32 ms exposure time). All imaging data were analyzed after background subtraction using ImageJ. To control the local atmosphere and humidity around the sample, a custom-built enclosed chamber (with inlets for appropriate gas and water vapor) was attached onto the sample stage. PL microscopy of perovskite microcrystals was conducted in the closed chamber where the moisturized gas was purged through a flow meter and the humidity inside was monitored using a relative humidity (RH) sensor (schematic of the entire setup is shown in Figure S10). All measurements were performed at 295 K.

RESULTS AND DISCUSSION

All our measurements, unless otherwise mentioned, were performed under controlled surrounding ambient conditions and recorded under illumination for 60 s. The spectroscopic investigations were performed on the same set of microcrystals with varying RH. Usually, the time taken to increase the RH by 10% is ca. 5 min, and during this period, the material is kept under the dark.

Effect of Moisture on PL Intensity. It is comprehended from the literature that moisture interacts reversibly and irreversibly with hybrid perovskite materials.[12−14] Our investigation here is directed to understand the electronic heterogeneity that is instantaneously created on the microcrystals of $MAPbBr_3$ under highly controlled moisture exposure. Figure 1a shows the PL image of a cluster of $MAPbBr_3$ microcrystals obtained under 15−20% RH. The morphology of the grains obtained from the PL images here is in reciprocation to that obtained from SEM, as shown in Figure S3. In this humidity region (15−20% RH), a continuous increase in the PL intensity of the perovskite microcrystals is observed (Figures 1h and S4). The gradual increase in the PL intensity can be attributed to the light-induced passivation of the nonradiative intrinsic defect states similar to the one reported earlier,[15,16] often termed as *photocuring* (vide infra). Upon further increase in the RH of the surrounding ambience to 35−40%, no considerable change in the PL intensity is noted, indicating that the photoactivation process has reached saturation in that stipulated time period. However, a substantial decrease in the PL intensity is observed when the RH is further increased to ca. 55−60%. Additional increase in the RH results in a further decrease in the PL intensity, as illustrated in Figure 1c−f. The PL images of the particular microcrystal shown under different humidity conditions are the average of PL intensity of all time frames

DOI: 10.1021/acs.jpcc.8b03862
J. Phys. Chem. C 2018, 122, 15133−15139

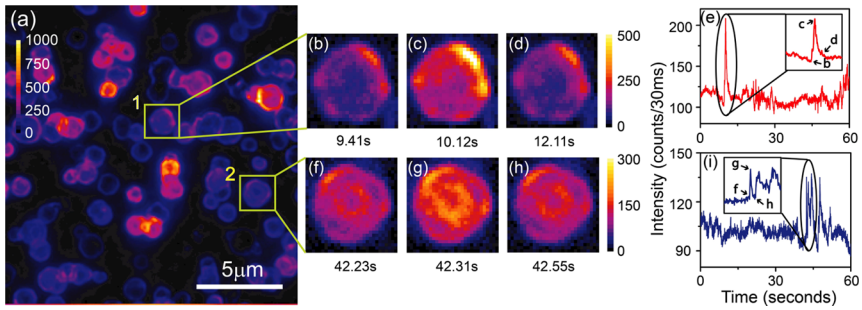

Figure 2. PL flickering behavior of $MAPbBr_3$ perovskite microcrystals in air at higher RH (≥75%). (a) Average PL image of a cluster of microcrystals recorded over 60 s. The flickering behavior of the microcrystals marked 1 and 2 is elaborated alongside. (b–d) and (f–h) represent the PL images of the microcrystals 1 and 2, respectively, at their sudden *bright* states. The corresponding PL intensity time traces are shown in (e,i). In the insets, the particular positions of (b–d,f–h) are demonstrated in their respective PL intensity time traces.

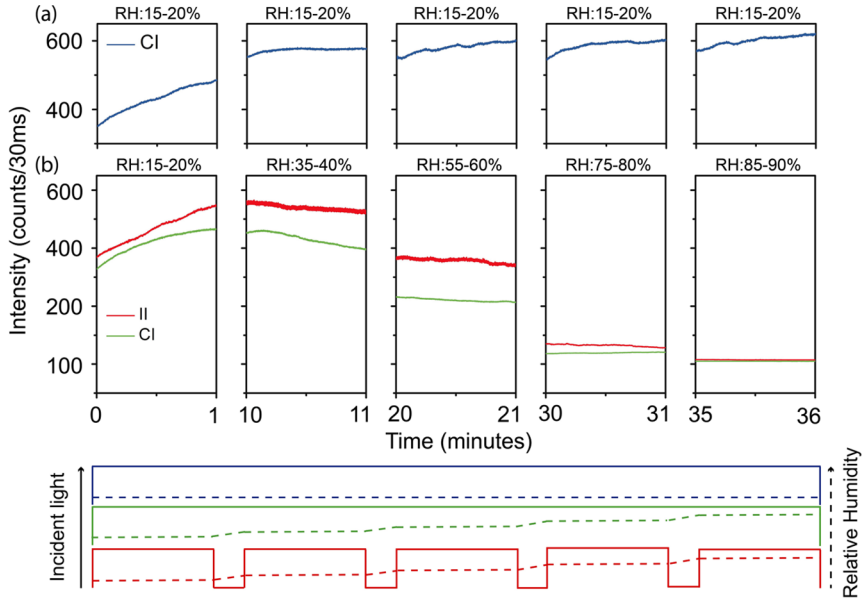

Figure 3. Effect of photoillumination on the PL of microcrystals in air at various RH values. (a) Average PL intensity time traces of the microcrystals under CI condition (blue) at constant 15–20% RH. (b) Average PL intensity time traces at CI (green) and II (red) under varied RH conditions. A schematic is shown below to emphasize the three experimental conditions with color code (CI in blue and green; II in red), where dashed lines indicate RH and solid lines represent the illumination condition (CI and II).

that are taken over 60 s (change of average PL intensity in a set of microcrystals is shown in Figure S5). In the bottom of every PL image, the corresponding PL intensity time traces (green) are also shown along with the average PL time trace of the entire cluster of microcrystals (red) (Figure 1i–m). The reduction of PL intensity with increasing RH can be attributed to the absorption/adsorption of water molecules on the hydrophilic hybrid perovskite materials[12,17] [no such detectable reduction of PL intensity at higher humidity is observed while replacing the organic cation with cesium ion (Cs^+) (Figure S6)]. Here, either or both of the following possibilities can play a deterministic role; (a) weakly bonded adsorbed water molecules can possibly create metastable trap states or (b) absorbed water molecules can react and thus degrade the material by releasing CH_3NH_2 and HBr.[18] Either of the scenario facilitates the nonradiative recombination processes in the perovskite microcrystals.

In addition to the above, it is also observed that the average PL intensity of the same set of microcrystals (that are already exposed to ca. 90% RH) get increased when the surrounding RH was reverted back to the lower value (15–20% RH), as shown in Figure 1g,m. We thus speculate that there is a reversible dehydration process, which initiates the partial recovery of the luminescence property of the microcrystals.[19] However, the individual intensity of the microcrystals was found substantially lower in comparison to that observed initially at ca. 15–20% RH, whereas some of the microcrystals turn out to be PL inactive (see Figures 1g and S7). The fractional reduction in the PL intensity of the individual microcrystal is also found to vary from one crystal to another.

PL Flickering of Entire Microcrystals. Interestingly, apart from the substantial lowering of the PL intensity under 75% (and higher) RH, a distinguishable temporal fluctuation in the PL is observed in $MAPbBr_3$ microcrystals. We observed such fluctuations both under controlled and regular ambient environments. These PL intensity fluctuations that extend more than a few frames are found to be slightly dissimilar to the ones that are often termed as "*blinking*," which is mostly seen in semiconductor nanocrystals [quantum dots (QDs)] and also in nanoparticles of halide perovskites where the temporal jump is usually abrupt and within one or two frames.[20,21] Here, the fluctuation of PL intensity is found to be

DOI: 10.1021/acs.jpcc.8b03862
J. Phys. Chem. C 2018, 122, 15133–15139

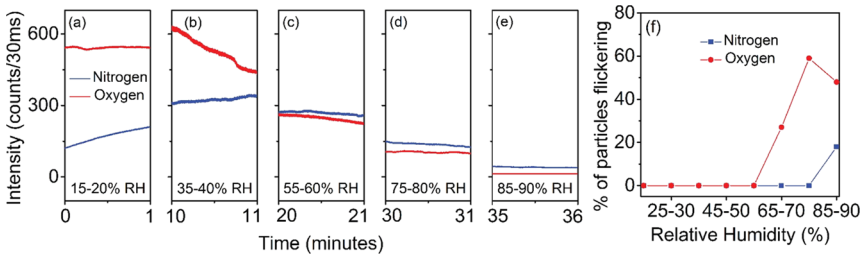

Figure 4. Effect of N_2/O_2 on the average PL intensity and flickering of 50 microcrystals upon II. (a–e) Average PL intensity time traces of perovskite microcrystals under different RH conditions under nitrogen (blue) and oxygen (red) atmospheres. (f) Number of microcrystals having flickering behavior among the total number of microcrystals illuminated under different RH conditions under nitrogen (blue) and oxygen (red).

a resultant of low-frequency fluctuations in combination with relatively higher frequency fluctuations. So, instead of clear "*on*" or "*off*" states traditionally obtained in blinking, multiple "*bright*" and "*dim*" states are observed in these microcrystals. We henceforth term the observed temporal PL intensity fluctuation as flickering only when the fluctuations in the PL intensity time trace between two consecutive frames differ by 5 times or higher than the standard deviation of the fluctuations. Figure 2 shows the pictorial demonstration of the PL flickering of the microcrystals alongside the time traces depicting the PL intensity fluctuations. At a high RH (≥75%) ambience, most of the time, enhancement of the PL intensity or "*bright*" state is observed. We note that in spite of having low-frequency fluctuations, such flickering behavior is not pronounced in perovskite crystals larger than few (ca. 5) micrometers. Such observations thus clearly differentiate between conventional blinking and flickering, as reported here.

As discussed earlier, the PL intensity of most of the microcrystals is fractionally recovered because the reversible desorption of moisture is observed when the RH of the ambient is reduced from high (ca. 90%) to low (15–20%). In addition to this, flickering behavior is also not observed at that particular condition. This clearly indicates that the permanent defect states introduced due to water-mediated degradation are not the only factors that induce the flickering in the microcrystals. It can be thus hypothesized that the flickering behavior can be initiated by the interplay between the permanent defect states created due to degradation and metastable defect states generated from reversible interaction of water molecules under higher RH conditions. It is important to mention that there was neither any change in the shape nor any shift in the spectra apart from the intensity that is found before and at the time of blinking (Figure S8). Such spectrally unchanged PL during the flickering process indicates that the recombination through low-lying traps is mostly insignificant.

Effect of Atmospheric Constituents and Light. Nonetheless, the effect of light cannot be denied here, which may activate either photoinduced or photo(electro)chemical effect in the process. To segregate these light-induced effects, we measured the average PL intensity time traces of an ensemble of microparticles under two different conditions, as shown in Figure 3;

(a) Continuous illumination (CI) under dry condition (ca. 15–20% RH) and
(b) Both CI and II under varied RH condition.

A characteristically different feature is observed in PL time trace upon CI at constant but low RH (15–20%) condition. No reduction in the PL intensity is detected throughout the course of this measurement, as depicted in Figure 3a. In the context of this article, it is important to note that the flickering in the PL intensity is evidently absent during long exposure in low RH even under CI. It certainly ascertains that the reduction in the PL intensity obtained under higher RH condition is mainly caused by the moisture in the surrounding atmosphere and not by the incident light.

Furthermore, the above experiment is repeated with changing humidity while keeping the material under CI. As can be seen from Figure 3b, under CI, the process of degradation gets substantially accelerated (green) with increased humidity in comparison to the one obtained under II (red). This observation implies that light can accelerate the moisture-induced degradation process. Because the degradation process is faster in the case of CI, PL flickering is observed in a relatively lower humidity (60–65%) level under CI than under II where the phenomenon is observed only beyond 75% RH. Thus, the flickering is found in consistent relation with the degradation history of the material.

To develop a comprehensive understanding to distinguish the contributory effect of the constituents of air on the optical properties of $MAPbBr_3$, a similar set of experiments with II were performed under nitrogen and oxygen atmospheres with varied humidity. At a lower RH (15–20%), the PL intensity is significantly higher when measured under oxygen atmosphere than in nitrogen ambience. Enhanced PL intensity under oxygen ambience is attributed to the passivation of intrinsic nonradiative defects by the Pb–O interaction.[21] Cycling the ambience between nitrogen and oxygen results in periodic changes in the PL intensity, indicating that the metal–oxygen interaction is not a permanent one. Upon increase in humidity, the relative decrease in the PL intensity with time is found comparatively faster under oxygen than in nitrogen. Because degradation is faster in oxygen atmosphere, blinking is evident above 60% RH, whereas in nitrogen, the phenomenon appears at ca. 85% RH, as shown in Figure 4f. The percentage of particles that show *flickering* is plotted against the RH of the surrounding, as shown in Figure 4f, whereas the average PL intensity time traces under different RH conditions are provided in Figure 4a–e. Interestingly, when the exposed material is taken back to 15–20% RH, the number of degraded particles is found to be less in nitrogen than in the oxygen atmosphere Figure S7.

Effect of Intrinsic Defects. As of now, we discuss the effect of extrinsically generated defects on the temporal PL properties of the microcrystals. In continuation, we opt to understand the involvement of intrinsic defects on the *flickering*. These intrinsic defects are those that exist inherently in the microcrystals upon synthesis. We have previously shown that upon illumination, the photogenerated charge carriers cure these defect states (i.e., *photocuring*) at 15–20% RH, and

DOI: 10.1021/acs.jpcc.8b03862
J. Phys. Chem. C 2018, 122, 15133–15139

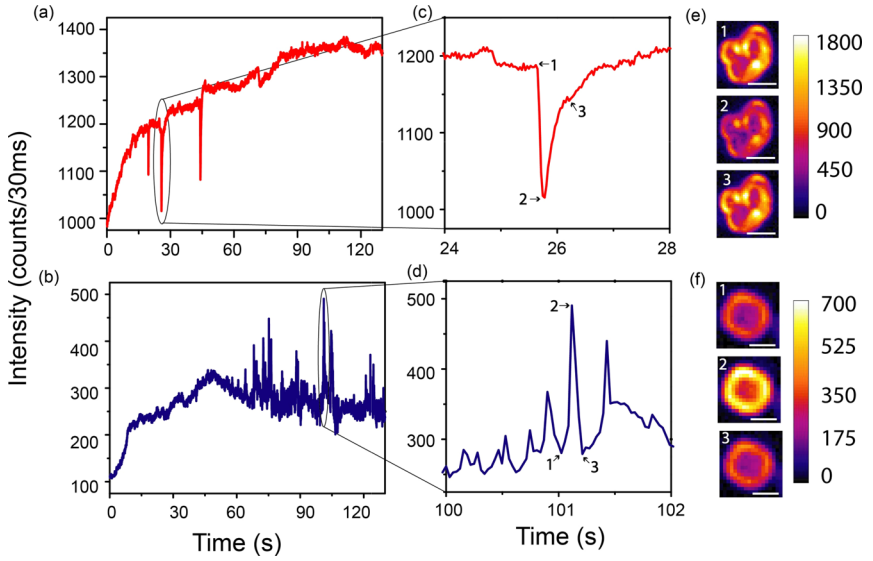

Figure 5. PL flickering of *photo-uncured* $MAPbBr_3$ microcrystals under different humidity conditions. (a) Observation of sudden *dim* states in the PL intensity time trace under lower humidity conditions (35−70% RH). (b) Sudden *bright* states in the PL intensity time trace under higher humidity conditions (75−90% RH). (c,d) Emphasize the *dim* and *bright* states in the corresponding PL intensity time traces, marked with a black circle. The PL images of the particular microcrystals at positions 1, 2, and 3 in (c,d) are shown in (e,f), respectively. The white line showed in PL images indicates 1 μm.

then measurements under higher humidity conditions are performed on the same set of microcrystals. In contrast to the above, for each measurement, a new set of unexposed microcrystals is studied under different RH values. In the absence of any *photocuring*, the flickering phenomenon starts at a relatively lower humidity (35%), as shown in the PL intensity time trace (Figure S9b−d). The striking difference between the *flickering* that is observed under high RH in photocured samples and here is the directional reversal of the *flickering* behavior. Figure 5a,c,e shows the PL intensity time trace and the corresponding PL image of the microparticles that undergoes *flickering* from a normally *bright* state to a momentarily *dim* state. To be noted here is that when the same experiment is performed at a higher humidity, the flickering direction goes from the normally dim state to the sudden bright state, as shown in Figure 5b,d,f (also in Figure S9e,f). This is similar to the ones discussed earlier in photocured samples. Under inadequate experimental evidences, we refrain from establishing a direct correlation between the nature of the intrinsic defect states and the PL flickering, though it exists. It may be a subject of further investigation. We thus like to emphasize on the fact that the flickering can be seen under a microscope, but the directional nature of PL time trace is important to understand the nature of the material.

DISCUSSIONS

PL properties can be a resultant of two competitive recombination processes: radiative and nonradiative; here, the intrinsic defect density and distribution play a deterministic role. On the other hand, the PL intermittency is truly a dynamic process where relative changes in the defect density temporally suppress either the radiative or nonradiative process, resulting in impulsive enhancement or reduction in the PL intensity. For example, in the nanocrystalline materials, preferential trapping of the photogenerated charge carriers in the metastable states initiates the nonradiative Auger process. This process effectively suppressed all radiative processes, resulting in temporal reduction of the PL intensity. However, the relatively short lifetime (ca. 2 ns) of these states[20] results in reversion to the radiative state, and thus the process continues between the PL active (ON) and inactive (OFF) states. By contrast, our observation that is described in this work (also summarized in Table S11, Supporting Information) where PL flickering is observed in micron size perovskite particle is likely to be different from what is traditionally referred as blinking. The net photon absorption (1 W cm^{-2}) in these microparticles is not enough to boost the carrier concentration to the Auger limit, as also shown by Merdasa et al.[5] Here, the fluctuation in PL is not a digital ON/OFF system, rather the variation in the intensity is observed as an additive effect on top of the overall PL background. In larger crystals, the photoexcited carrier dynamics is diffusion-limited and not simply governed by the thermal velocity as in QDs or nanosize domains within microcrystals. It is thus possible that in the vicinity of sufficient number of metastable defects, the photogenerated charge-carrier pairs non-radiatively recombine. However, because of the high mobility of both type of charge carriers, it is inherently not localized. Nevertheless, if the sizes of the crystals are way bigger than the average diffusion length of the charge carriers, then localized PL intermittency is observed, as we have previously shown.[6] As it can be understood that the abovementioned process does not affect the majority of the charge carrier pairs, the net bulk radiative recombination is unaltered, which is responsible for the background PL.

Furthermore, to initiate the flickering, a relatively higher surface defect density is desirable instead of single trap states that are often needed in QDs because of a substantially lower surface-to-volume ratio.[21] By now, the energetic nature of these trap states is not classified, but our experimental observations clearly assert the fact that these trap states are generated through photo(electro)chemical processes involving water molecules. Here, the chemical nature of the material and the surface property play a deterministic role. We believe that the weak hydrogen bonding can be a dynamic process resulting in temporal formation and/or deformation of surface states

DOI: 10.1021/acs.jpcc.8b03862
J. Phys. Chem. C 2018, 122, 15133−15139

along with the permanent defect states that initiate nonradiative or radiative recombination pathway. However, our observation probably indicates that the flickering process is not initiated by a single quenching site, rather by a concerted phenomenon, as the raise or decay in PL is not abrupt and recorded over more than a couple of frames. A phenomenological model of the observation depicting the flickering process has been communicated separately.[22]

CONCLUSIONS

Using epi-fluorescence video microscopy, we investigated the effect of ambience and photoillumination on the PL flickering of whole micron-sized crystals (ca. 1−2 μm) of $MAPbBr_3$, an unprecedented phenomenon that is noticeably different from the conventional blinking in nanoparticles. We find that flickering of PL intensity primarily depends on the RH of the ambience and the hydrophilic nature of the cation. Our results indicate that PL intermittency is associated with the reduction in the emission quantum yield, as expected for degradation of the material, and such processes slow down under an inert environment at comparable RH. The adsorbed moisture initiates both irreversible photo(electro)chemical reaction and reversible (adsorption) interaction, which leads to the formation of permanent and metastable nonradiative defects, respectively. Interestingly, for *photocured* microcrystals, the flickering generally occurs from *dim* states to intermittent short-lived *bright* states, which we attribute to transient removal metastable defects. However, the process reverses in *non-photocured* materials, and apparently, the flickering occurs at relatively lower humidity than the preceding, primarily due to the intrinsic defects in the materials. As the reduction of the PL intensity is a qualitative measure of degraded perovskite materials, we infer that PL flickering marks the onset of moisture and/or oxygen-induced degradation of hybrid perovskites.

ASSOCIATED CONTENT

Supporting Information

The Supporting Information is available free of charge on the ACS Publications website at DOI: 10.1021/acs.jpcc.8b03862.

XRD of $MAPbBr_3$ perovskite microcrystals deposited on a coverslip, UV−vis and PL spectroscopy of perovskite microcrystals deposited on a coverslip, surface SEM image and cross-sectional SEM image of perovskite microcrystals deposited on a glass coverslip, average PL images of a set of microcrystals in air at the specified humidity conditions, average PL intensity time traces of $CsPbBr_3$ microcrystals in air under different humidity conditions, average PL image of perovskite microcrystals at 15−20% RH under nitrogen, air, and oxygen atmospheres, PL spectra of the same microcrystal before the occurrence of PL flickering and at the flickering condition, PL intensity time traces of $MAPbBr_3$ microcrystals when new set of microcrystals are illuminated, schematic of the home-built wide-field microscopy setup with a chamber for humidity control experiments, and table summarizing the condition of flickering under different conditions described in the manuscript (PDF)

AUTHOR INFORMATION

Corresponding Authors

*E-mail: arindam@chem.iitb.ac.in (A.C.).
*E-mail: shaibal.sarkar@iitb.ac.in (S.K.S.).

ORCID

Arindam Chowdhury: 0000-0001-8178-1061
Shaibal K. Sarkar: 0000-0001-6788-9738

Author Contributions

§A.H. and N.P. contributed equally.

Notes

The authors declare no competing financial interest.

ACKNOWLEDGMENTS

This article is based upon the work supported under the US-India Partnership to Advance Clean Energy-Research (PACE-R) for the Solar Energy Research Institute for India and the United States (SERIIUS), funded jointly by the U.S. Department of Energy (Office of Science, Office of Basic Energy Sciences, and Energy Efficiency and Renewable Energy, Solar Energy Technology Program, under subcontract DE-AC36-08GO28308 to the National Renewable Energy Laboratory, Golden, Colorado) and the Government of India, through the Department of Science and Technology under subcontract IUSSTF/JCERDC-SERIIUS/2012 dated 22nd November 2012. This work is also partially supported by the Ministry of New and Renewable Energy (MNRE), Government of India.A.C. thanks the National Centre for Photovoltaic Research and Education (NCPRE) at IIT Bombay, funded by MNRE, Government of India, for the partial support.

REFERENCES

(1) Yang, W. S.; Park, B.-W.; Jung, E. H.; Jeon, N. J.; Kim, Y. C.; Lee, D. U.; Shin, S. S.; Seo, J.; Kim, E. K.; Noh, J. H.; Seok, S. I. Iodide Management in Formamidinium-Lead-Halide−based Perovskite Layers for Efficient Solar Cells. *Science* **2017**, *356*, 1376−1379.

(2) Correa-Baena, J.-P.; Saliba, M.; Buonassisi, T.; Grätzel, M.; Abate, A.; Tress, W.; Hagfeldt, A. Promises and Challenges of Perovskite Solar Cells. *Science* **2017**, *358*, 739−744.

(3) Leijtens, T.; Bush, K.; Cheacharoen, R.; Beal, R.; Bowring, A.; McGehee, M. D. Towards Enabling Stable Lead Halide Perovskite Solar Cells; Interplay between Structural, Environmental, and Thermal Stability. *J. Mater. Chem. A* **2017**, *5*, 11483−11500.

(4) de Quilettes, D. W.; Vorpahl, S. M.; Stranks, S. D.; Nagaoka, H.; Eperon, G. E.; Ziffer, M. E.; Snaith, H. J.; Ginger, D. S. Impact of Microstructure on Local Carrier Lifetime in Perovskite Solar Cells. *Science* **2015**, *348*, 683−686.

(5) Merdasa, A.; Tian, Y.; Camacho, R.; Dobrovolsky, A.; Debroye, E.; Unger, E. L.; Hofkens, J.; Sundström, V.; Scheblykin, I. G. "Supertrap" at Work: Extremely Efficient Nonradiative Recombination Channels in $MAPbI_3$ Perovskites Revealed by Luminescence Super-Resolution Imaging and Spectroscopy. *ACS Nano* **2017**, *11*, 5391−5404.

(6) Halder, A.; Chulliyil, R.; Subbiah, A. S.; Khan, T.; Chattoraj, S.; Chowdhury, A.; Sarkar, S. K. Pseudohalide (SCN−)-Doped $MAPbI_3$ Perovskites: A Few Surprises. *J. Phys. Chem. Lett.* **2015**, *6*, 3483−3489.

(7) Tian, Y.; Merdasa, A.; Peter, M.; Abdellah, M.; Zheng, K.; Ponseca, C. S.; Pullerits, T.; Yartsev, A.; Sundström, V.; Scheblykin, I. G. Giant Photoluminescence Blinking of Perovskite Nanocrystals Reveals Single-Trap Control of Luminescence. *Nano Lett.* **2015**, *15*, 1603−1608.

(8) Seth, S.; Mondal, N.; Patra, S.; Samanta, A. Fluorescence Blinking and Photoactivation of All-Inorganic Perovskite Nanocrystals $CsPbBr_3$ and $CsPbBr_2I$. *J. Phys. Chem. Lett.* **2016**, *7*, 266−271.

DOI: 10.1021/acs.jpcc.8b03862
J. Phys. Chem. C 2018, 122, 15133−15139

(9) Galland, C.; Ghosh, Y.; Steinbrück, A.; Sykora, M.; Hollingsworth, J. A.; Klimov, V. I.; Htoon, H. Two Types of Luminescence Blinking Revealed by Spectroelectrochemistry of Single Quantum Dots. *Nature* **2011**, *479*, 203−207.
(10) Yuan, H.; Debroye, E.; Caliandro, G.; Janssen, K. P. F.; van Loon, J.; Kirschhock, C. E. A.; Martens, J. A.; Hofkens, J.; Roeffaers, M. B. J. Photoluminescence Blinking of Single-Crystal Methylammonium Lead Iodide Perovskite Nanorods Induced by Surface Traps. *ACS Omega* **2016**, *1*, 148−159.
(11) Wen, X.; Ho-Baillie, A.; Huang, S.; Sheng, R.; Chen, S.; Ko, H.-c.; Green, M. A. Mobile Charge-Induced Fluorescence Intermittency in Methylammonium Lead Bromide Perovskite. *Nano Lett.* **2015**, *15*, 4644−4649.
(12) Salado, M.; Contreras-Bernal, L.; Caliò, L.; Todinova, A.; López-Santos, C.; Ahmad, S.; Borras, A.; Idígoras, J.; Anta, J. A. Impact of Moisture on Efficiency-Determining Electronic Processes in Perovskite Solar Cells. *J. Mater. Chem. A* **2017**, *5*, 10917−10927.
(13) Zhao, X.; Park, N.-G. Stability Issues on Perovskite Solar Cells. *Photonics* **2015**, *2*, 1139−1151.
(14) Tong, C.-J.; Geng, W.; Tang, Z.-K.; Yam, C.-Y.; Fan, X.-L.; Liu, J.; Lau, W.-M.; Liu, L.-M. Uncovering the Veil of the Degradation in Perovskite $CH_3NH_3PbI_3$ upon Humidity Exposure: A First-Principles Study. *J. Phys. Chem. Lett.* **2015**, *6*, 3289−3295.
(15) Tian, Y.; Peter, M.; Unger, E.; Abdellah, M.; Zheng, K.; Pullerits, T.; Yartsev, A.; Sundström, V.; Scheblykin, I. G. Mechanistic Insights into Perovskite Photoluminescence Enhancement: Light Curing with Oxygen Can Boost Yield Thousandfold. *Phys. Chem. Chem. Phys.* **2015**, *17*, 24978−24987.
(16) Mosconi, E.; Meggiolaro, D.; Snaith, H. J.; Stranks, S. D.; De Angelis, F. Light-Induced Annihilation of Frenkel Defects in Organo-Lead Halide Perovskites. *Energy Environ. Sci.* **2016**, *9*, 3180−3187.
(17) Ahn, N.; Kwak, K.; Jang, M. S.; Yoon, H.; Lee, B. Y.; Lee, J.-K.; Pikhitsa, P. V.; Byun, J.; Choi, M. Trapped Charge-Driven Degradation of Perovskite Solar Cells. *Nat. Commun.* **2016**, *7*, 13422.
(18) Frost, J. M.; Butler, K. T.; Brivio, F.; Hendon, C. H.; van Schilfgaarde, M.; Walsh, A. Atomistic Origins of High-Performance in Hybrid Halide Perovskite Solar Cells. *Nano Lett.* **2014**, *14*, 2584−2590.
(19) Leguy, A. M. A.; Hu, Y.; Campoy-Quiles, M.; Alonso, M. I.; Weber, O. J.; Azarhoosh, P.; van Schilfgaarde, M.; Weller, M. T.; Bein, T.; Nelson, J.; et al. Reversible Hydration of $CH_3NH_3PbI_3$ in Films, Single Crystals, and Solar Cells. *Chem. Mater.* **2015**, *27*, 3397−3407.
(20) Nirmal, M.; Dabbousi, B. O.; Bawendi, M. G.; Macklin, J. J.; Trautman, J. K.; Harris, T. D.; Brus, L. E. Fluorescence Intermittency in Single Cadmium Selenide Nanocrystals. *Nature* **1996**, *383*, 802−804.
(21) Tachikawa, T.; Karimata, I.; Kobori, Y. Surface Charge Trapping in Organolead Halide Perovskites Explored by Single-Particle Photoluminescence Imaging. *J. Phys. Chem. Lett.* **2015**, *6*, 3195−3201.
(22) Pathor, N.; Halder, A.; Mukherjee, A.; Mahato, J.; Sarkar, S. K.; Chowdhury, A.. Fluorescence blinking beyond nano-confinement: Spatially synchronous intermittency of entire perovskite micro-crystals, DOI: 10.1002/anie.201804852 and DOI: 10.1002/ange.201804852.

■ NOTE ADDED AFTER ASAP PUBLICATION

This paper was published to the Web on June 27, 2018, with errors in the TOC and abstract graphics and ref 22. These were corrected in the version published to the Web on June 29, 2018.

DOI: 10.1021/acs.jpcc.8b03862
J. Phys. Chem. C 2018, 122, 15133−15139